experimental error, the same emission lifetime. The value τ = 85 μs is much lower than that of the free ligand ($\tau > 10^5$ μs) and that of the complex in glasses (τ = 2600 μs) at T = 77 K[6] and 7 K.[22] These differences are probably caused by different spin-orbit couplings due to a weak admixture of the metal orbital $1a_2(xy)$ to the HOMO of the complex and by an intercomplex coupling in the crystal, respectively.

Raising the temperature depletes the X-trap states and populates the exciton band. According to the strong temperature dependence of the detrapping rates k_{so}, k_{do} and to the distinct stabilization energies ΔE_s, ΔE_d the depopulation of the different X-trap types starts at different temperatures. With increasing temperature first the shallow X-traps are deactivated ($k_{so} \neq 0$, $k_{do} \approx 0$) and the corresponding 0-0 transitions (and their vibronic satellites) of the emission spectra vanish. The simultaneous loss of the monoexponential character of the decay and the reduction of the emission lifetime of the shallow-trap states are accomplished by the competing mechanisms of detrapping and trapping. At further temperature increase to $T \approx 60$ K thermal equilibrium is established between all X-traps, with the exception of the deepest one ($\Delta E_d \approx 780$ cm^{-1}), and the exciton band. For this reason the 60 K emission spectra consist only of the deep-trap emission. The observed reduction of the integral emission intensity between T = 5 and 60 K is probably due to the inefficiency of the system in transferring the total excitation energy via the exciton band to the deep traps, and there exists rather a nonradiative deactivation with a temperature-dependent rate.

To describe the temperature dependence of the detrapping processes, a quantitative model developed by Fayer and Harris[23,24] can be applied. In this model the detrapping rate k_{so} of a shallow trap varies with temperature as $k_{so} = k_{so}^0 e^{-\Delta E_s/kT}$ with ΔE_s being the stabilization energy. If there exist deeper traps (stabilization energies ΔE_d) coupled to the shallow traps via the exciton band, then the logarithmic plot of the intensity ratio

$$\frac{I_d}{I_s} = \frac{N_d}{N_s} \frac{k_s + k_{so}^0 e^{-\Delta E_s/kT}}{k_d + k_{do}}$$

versus the reciprocal temperature $1/T$ is composed of two parts. N_d and N_s are the numbers of the traps, and I_d and I_s represent the emission intensities of the deep and the shallow traps, respectively. At temperatures too low to depopulate the shallow traps and the deep traps (k_{so}, k_{do} = 0; $k_s \approx k_d$), the intensity ratio is constant and reflects the ratio of the numbers of deep and of shallow traps. In the temperature range that allows the detrapping of the shallow traps but not of the deep traps ($k_{so} \gg k_s$; k_{do} = 0), ln (I_d/I_s) varies as $-\Delta E_s/kT$. The slope of the plot of ln (I_d/I_s) versus $1/T$ yields the trap depth ΔE_s. Experiments of this kind with crystalline organic compounds have been reported in ref 25-28.

If the emission lines labeled by the numbers 2 and 3 in Figure 4 are assigned to shallow traps and deep traps, respectively, the graph in Figure 7 is in agreement with the theoretical predictions. From Figure 7 the value of the stabilization energy ΔE_s can be calculated as $\sim$177 cm^{-1}. That harmonizes well with the experimental energy gap of $\Delta\bar{\nu} < 204$ cm^{-1} between the emission peak 2 and the low-energy absorption band.

With excitation wavelength λ_{exc} = 488 nm a selective excitation of X-traps of type 4 results. At T = 1.9 K a thermally activated energy transfer from these traps into the exciton band is suppressed and, therefore, all traps of other type remain in their electronic ground state. For this reason the emission spectrum consists only of the trap 4 emission and it differs distinctly from the 1.9 K spectrum with UV excitation. Raising the temperature causes an efficient detrapping of the X-traps of type 4. The corresponding energy is transferred rapidly via the exciton band and finally localized at X-traps again. At T = 50 K all traps with the exception of the deepest one ($\Delta E \approx 780$ cm^{-1}) are in thermal equilibrium with the exciton band and, therefore, the 50 K emission spectrum is assigned to originate from the deepest traps.

Acknowledgment. This research has been supported by the Deutsche Forschungsgemeinschaft, the Fonds der Chemischen Industrie, and the Swiss National Science Foundation.

Contribution from the Christopher Ingold Laboratories, University College London, 20 Gordon Street, London WC1H 0AJ, England

Electronic, Infrared, Raman, and Resonance Raman Spectra of the Dirhodium Tetracarboxylate Complexes $Rh_2(O_2CR)_4(PPh_3)_2$ (R = H, CH_3, C_2H_5, C_3H_7)

Robin J. H. Clark* and Andrew J. Hempleman

Received May 10, 1988

The electronic spectra of the series of complexes $Rh_2(O_2CR)_4(PPh_3)_2$ (R = H, CH_3, C_2H_5, C_3H_7) are characterized by a strong absorption ($\lambda_{max} \approx 380$ nm) of essentially $\sigma(Rh_2) \rightarrow \sigma^*(Rh_2)$ character. Excitation within the contour of this band leads to resonance Raman spectra that are dominated by a band progression in ν(RhRh). Both resonance Raman and Raman (514.5 nm) spectra have been obtained for the complexes with R = H, C_2H_5, C_3H_7, and these are compared to those previously reported for $Rh_2(O_2CCH_3)_4(PPh_3)_2$. While ν_1 (ν(RhRh)) occurs at 292 $\pm$ 7 cm^{-1} over all four complexes, the band attributed to the totally symmetric ν(RhO) vibration, ν_2, is shown to be strongly dependent on the mass of the R group, occurring at 402, 338, 310, and 289 cm^{-1} for the complexes with R = H, CH_3, C_2H_5, and C_3H_7, respectively. The intensity ratio $I(\nu_2)/I(\nu_1)$ and the length of the overtone progressions in ν_2 are shown to be dependent upon the wavenumber separation ν(RhO) - ν(RhRh). FTIR spectra (3500-40 cm^{-1}) are also assigned.

Introduction

For dimetal tetracarboxylates of the type $M_2(O_2CR)_4L_2$, changes in the carboxylate bridging ligand usually have little effect upon ν(MM) if the axial ligands either are absent or are kept constant. Thus, for the series $Mo_2(O_2CR)_4$ (R = H, CH_3, C_2H_5, C_3H_7, C_6H_5, C_6H_{11}, CF_3, CH_2Cl, $CHCl_2$, CCl_3) ν(MoMo) is found in the range 406-395 cm^{-1} [1-8] and for the series $Ru_2(O_2CR)_4Cl$ (R = H, CH_3, C_2H_5, C_3H_7) ν(RuRu) is found in the range 339-327 cm^{-1}.[6,9] This relative insensitivity of ν(MM) to change of R is a reflection of the lack of mixing between the R group and M-M symmetry coordinates as well as of the small

* To whom correspondence should be addressed.

(1) Cotton, F. A.; Norman, J. G., Jr.; Stults, B. R.; Webb, T. R. *J. Coord. Chem.* **1976**, *5*, 217.
(2) Hutchinson, B.; Morgan, J.; Cooper, C. B., III; Mathey, Y.; Shriver, D. F. *Inorg. Chem.* **1979**, *18*, 2048.
(3) Bratton, W. K.; Cotton, F. A.; Debeau, M.; Walton, R. A. *J. Coord. Chem.* **1971**, *1*, 121.
(4) Clark, R. J. H.; Hempleman, A. J.; Kurmoo, M. *J. Chem. Soc., Dalton Trans.* **1988**, 973.
(5) Ketteringham, A. P.; Oldham, C. *J. Chem. Soc., Dalton Trans.* **1973**, 1067.
(6) San Filippo, J., Jr.; Sniadoch, H. J. *Inorg. Chem.* **1973**, *12*, 2326.

0020-1669/89/1328-0746$01.50/0 © 1989 American Chemical Society

variation in r(M–M) with the carboxylate R group. For example, in the complexes $Mo_2(O_2CR)_4$ (R = H, CH_3, CF_3, CMe_3, C_6H_5) r(Mo–Mo) is found in the range 2.096–2.088 Å[10] and for the series $Ru_2(O_2CR)_4Cl$ (R = CH_3, C_2H_5, C_3H_7) r(Ru–Ru) is found in the range 2.292–2.267 Å.[10]

In making assignments of ν(MM) for dimeric tetracarboxylates, it is important to distinguish between bands arising from ν(MM) and ν(MO) modes, as both often occur in the same spectral region. Unfortunately most researchers have almost exclusively confined their studies to ν(MM) and have not reported other bands in the spectra, in particular those attributable to ν(MO). The only species for which data are available on the variation of ν(MO) with R group is $Ru_2(O_2CR)_4Cl$ (R = H, CH_3, C_2H_5, C_3H_7).[9] For these complexes ν(RuO) is assigned to Raman bands at 432, 372, 395, and 377 cm^{-1} for the complexes with R = H, CH_3, C_2H_5, and C_3H_7, respectively;[9] an alternative assignment of ν(RuO) for the butyrate to a band at 435 cm^{-1} has recently been proposed.[11] However, for either assignment the variation in ν(RuO), 60 cm^{-1}, is much larger than that, 12 cm^{-1}, observed for ν(RuRu).

In contrast to the situation for the complexes $Rh_2(O_2CCH_3)_4L_2$ (L = PPh_3, $AsPh_3$, $SbPh_3$, $S(CH_2Ph)_2$),[12-15] for which ν(RhRh) is identified with the band that shifts on change of L, for the present complexes ν(RhRh) is expected to be relatively insensitive to a change in the carboxylate alkyl group. Obviously the assignments rely on the satisfactory identification of bands due to the axial ligands.[16]

The four complexes under study are $Rh_2(O_2CR)_4(PPh_3)_2$ (R = H, CH_3, C_2H_5, C_3H_7), these being chosen because both resonance and off-resonance Raman spectra were obtainable. Some band assignments have already been made for $Rh_2(O_2CCH_3)_4(PPh_3)_2$.[12,13]

Experimental Section

Preparation of Complexes. $Rh_2(O_2CCH_3)_4(PPh_3)_2$ was prepared and analyzed as described previously.[13] Samples of $Rh_2(O_2CR)_4(PPh_3)_2$ (R = H, C_2H_5, C_3H_7) were prepared by an analogous procedure using the desired dirhodium tetracarboxylate as the starting material. Anal. Calcd for $Rh_2(O_2CH)_4(PPh_3)_2$: C, 52.8; H, 3.76; P, 6.80. Found: C, 52.4; H, 3.71; P, 6.62. Calcd for $Rh_2(O_2CC_2H_5)_4(PPh_3)_2$: C, 56.4; H, 4.93; P, 6.06. Found: C, 56.2; H, 4.88; P, 6.39. Calcd for $Rh_2(O_2CC_3H_7)_4(PPh_3)_2$: C, 57.9; H, 5.42; P, 5.74. Found: C, 57.9; H, 5.37; P, 6.04.

Instrumentation. Raman spectra of the complexes were recorded with a Spex 14018 (R6) spectrometer in the double-monochromator mode, in conjunction with Coherent CR 3000 K and CR 12 lasers. The Raman spectra with 514.5-nm excitation were also obtained in the triple-monochromator mode for the region <400 cm^{-1}. Raman samples were held as pressed KCl disks at ca. 80 K by using a liquid-nitrogen-cooled cell and at ca. 15 K by using an Air Products Displex system.

Infrared spectra were recorded with a Bruker 113V interferometer at a spectral resolution of 1 cm^{-1}. Samples were recorded as KCl disks (3500–500 cm^{-1}) and as wax disks (660–40 cm^{-1}) and held at ca. 80 K by using a liquid-nitrogen-cooled cryostat.

Solid-state transmission electronic spectra were obtained on KCl disks of the complexes at ca. 20 K by using an Air Products Displex system in conjunction with a Cary 14 spectrometer. Solution measurements were made with dichloromethane as solvent on a Perkin-Elmer λ5G spectrometer. Band maxima (nm) and extinction coefficients (M^{-1} cm^{-1}, in parentheses) are as follows. $Rh_2(O_2CH)_4(PPh_3)_2$: solid ~272 sh, 320 m, 380 s, ~490 w; solution, 375 (45 300), ~500 (~1400). $Rh_2(O_2CCH_3)_4(PPh_3)_2$: solid ~271 sh, 318 m, 376 s, ~479 m, sh; solution, 365 (39 900), ~505 (~920). $Rh_2(O_2CC_2H_5)_4(PPh_3)_2$: solid ~274 sh, 319 m, 382 s, ~491 m, sh; solution, 366 (43 500), ~500 (~1100). $Rh_2(O_2CC_3H_7)_4(PPh_3)_2$: solid ~272 sh, 320 m, 376 s, ~476 m, sh; solution, 366 (43 400), ~500 (~1200).

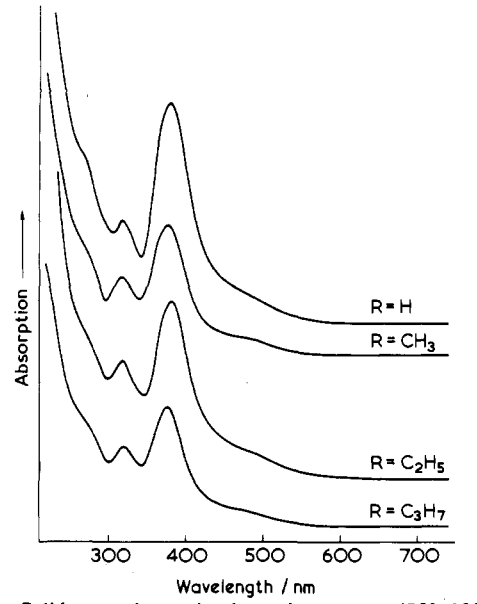

Figure 1. Solid-state electronic absorption spectra (750–220 nm) of $Rh_2(O_2CR)_4(PPh_3)_2$ (R = H, CH_3, C_2H_5, C_3H_7) as KCl disks at ca. 20 K.

Results and Discussion

Electronic Spectra. The transmission spectra of the complexes $Rh_2(O_2CR)_4(PPh_3)_2$ (R = H, CH_3, C_2H_5, C_3H_7) in the solid state at ca. 20 K are shown in Figure 1. The band maxima and extinction coefficients show little dependence on the alkyl substituent. Thus, the band maxima in the near-UV region occur at 375, 365, 366, and 366 nm for the complexes with R = H, CH_3, C_2H_5, and C_3H_7, respectively, the extinction coefficients being 45 300, 39 900, 43 500, and 43 400 M^{-1} cm^{-1}, respectively. There is also a shoulder at ca. 500 nm for all four complexes with an extinction coefficient of ca. 1000 M^{-1} cm^{-1}.

Sowa et al.[17] have investigated the solution electronic spectra of the complexes $Rh_2(O_2CR)_4(PPh_3)_2$ (R = C_2H_5, CF_3) and of some cation radicals derived therefrom. The spectrum obtained here for $Rh_2(O_2CC_2H_5)_4(PPh_3)_2$ is in good agreement with that of Sowa et al.,[17] who identified an intense absorption band at 27 300 cm^{-1} and a much weaker one around 20 000 cm^{-1}. The transitions of lowest wavenumber for $Rh_2(O_2CH)_4(PH_3)_2$ have been predicted by Bursten and Cotton[18] to be $\sigma(Rh_2)$, $\sigma^*(RhP) \rightarrow \sigma^*(RhO)$ at 14 800 cm^{-1} and $\sigma(Rh_2)$, $\sigma^*(RhP) \rightarrow \sigma^*(Rh_2)$, $\sigma^*(RhP)$ at 16 400 cm^{-1} and to be separated from other allowed (in C_{2h}) transitions by about 10 000 cm^{-1}. Sowa et al.[17] have assigned the near-UV absorption band of the neutral dirhodium complexes to the $\sigma(Rh_2) \rightarrow \sigma^*(Rh_2)$ transition on intensity grounds.[19] However, the matter is not entirely clear since Bursten and Cotton's calculation[18] indicates that the HOMO has both σ(RhRh) and σ^*(RhP) character (but mainly the latter) whereas the ESR experiments[20,21] and the Hartree–Fock calculations[22,23] indicate that the HOMO is mainly based on the rhodium. Our results favor the latter assignment since the band wavelength is

(7) Cotton, F. A.; Norman, J. G., Jr. *J. Coord. Chem.* **1971**, *1*, 161.
(8) Holste, G. *Z. Anorg. Allg. Chem.* **1975**, *414*, 81.
(9) Clark, R. J. H.; Ferris, L. T. H. *Inorg. Chem.* **1981**, *20*, 2759.
(10) Cotton, F. A.; Walton, R. A. *Multiple Bonds Between Metal Atoms*; Wiley: New York, 1982.
(11) Miskowski, V. M.; Loehr, T. M.; Gray, H. B. *Inorg. Chem.* **1987**, *26*, 1098.
(12) Clark, R. J. H.; Hempleman, A. J.; Flint, C. D. *J. Am. Chem. Soc.* **1986**, *108*, 518.
(13) Clark, R. J. H.; Hempleman, A. J. *Inorg. Chem.* **1988**, *27*, 2225.
(14) Clark, R. J. H.; Hempleman, A. J. *Inorg. Chem.*, in press.
(15) Clark, R. J. H.; Hempleman, A. J. *J. Mol. Struct.*, in press.
(16) Clark, R. J. H.; Flint, C. D.; Hempleman, A. J. *Spectrochim. Acta* **1987**, *43A*, 805.
(17) Sowa, T.; Kawamura, T.; Shida, T.; Yonezawa, T. *Inorg. Chem.* **1983**, *22*, 56.
(18) Bursten, B. E.; Cotton, F. A. *Inorg. Chem.* **1981**, *20*, 3042.
(19) Abrahamson, H. B.; Frazier, C. C.; Ginley, D. S.; Gray, H. B.; Lilienthal, J.; Tyler, D. R.; Wrighton, M. S. *Inorg. Chem.* **1977**, *16*, 1554.
(20) Kawamura, T.; Fukamachi, K.; Hayashida, S. *J. Chem. Soc., Chem. Commun.* **1979**, 945.
(21) Kawamura, T.; Fukamachi, K.; Sowa, T.; Hayashida, S.; Yonezawa, T. *J. Am. Chem. Soc.* **1981**, *103*, 364.
(22) Nakatsuji, H.; Ushio, J.; Kanda, K.; Onishi, Y.; Kawamura, T.; Yonezawa, T. *Chem. Phys. Lett.* **1981**, *79*, 299.
(23) Nakatsuji, H.; Onishi, Y.; Ushio, J.; Yonezawa, T. *Inorg. Chem.* **1983**, *22*, 1623.

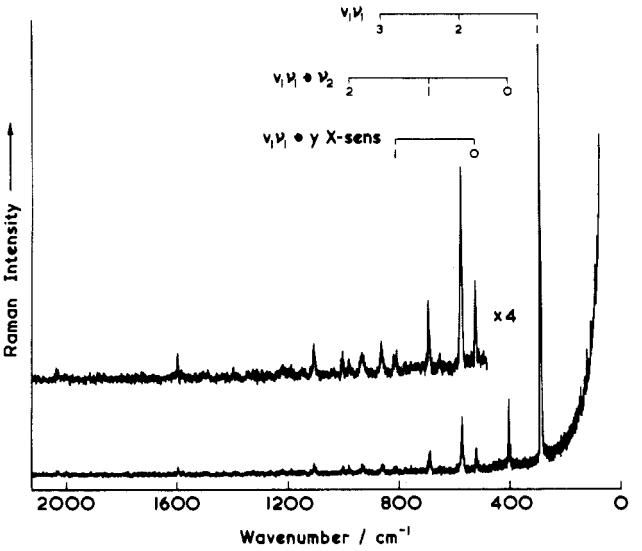

Figure 2. Resonance Raman spectrum (2100–60 cm^{-1}) of $Rh_2(O_2CH)_4(PPh_3)_2$ as a KCl disk at ca. 15 K with 406.7-nm excitation (resolution ca. 5 cm^{-1}).

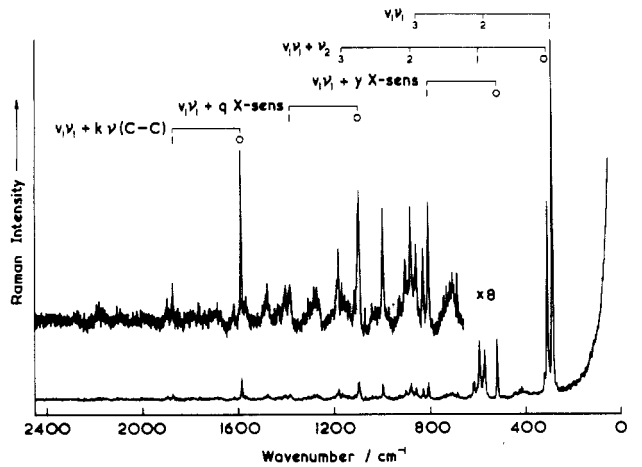

Figure 3. Resonance Raman spectrum (2450–40 cm^{-1}) of $Rh_2(O_2CC_2H_5)_4(PPh_3)_2$ as a KCl disk at ca. 15 K with 363.8-nm excitation (resolution ca. 5 cm^{-1}).

Table I. Wavenumbers (cm^{-1}) of Bands Observed in the Resonance Raman Spectrum[a] of $[Rh_2(O_2CH)_4(PPh_3)_2]$ at ca. 15 K

$\tilde{\nu}$	assignt	$\tilde{\nu}$	assignt
265 vw	u X-sens[b]	857 vw	$3\nu_1$
286 vs	ν_1, ν(RhRh)	928 vw, br	ν_2 + y X-sens
402 m	ν_2, ν(RhO)	975 vw	$2\nu_1 + \nu_2$
520 w	y X-sens	998 vw	p-ring
572 m	$2\nu_1$	1100 vw	q X-sens
649 vw		1142 vw	$4\nu_1$
688 w	$\nu_1 + \nu_2$	1210 vw, br	$\nu_1 + \nu_2$ + y X-sens
775 vw	δ(OCO)	1587 vw	k ν(CC)
808 vw	ν_1 + y X-sens		

[a] 406.7-nm excitation. [b] The nomenclature used is that of: Whiffen, D. H. *J. Chem. Soc.* **1956**, 1350.

approximately independent of axial donor atom M (λ_{max} values for MPh_3 complexes are 376, 352, and 361 nm for M = P, As, and Sb, respectively).[24] The lack of enhancement at resonance of any band attributable to ν(RhP) (vide infra) also suggests that the ca. 370 nm band has little phosphorus character to it. Moreover, the ρ value of the ν_1 (ν(RhRh)) band at resonance[12,13] (0.37) implies that the resonant transition is axially rather than equatorially polarized, a result that rules out significant σ(RhO) $\rightarrow$ $\sigma^*(Rh_2)$ character to the resonant electronic transition.

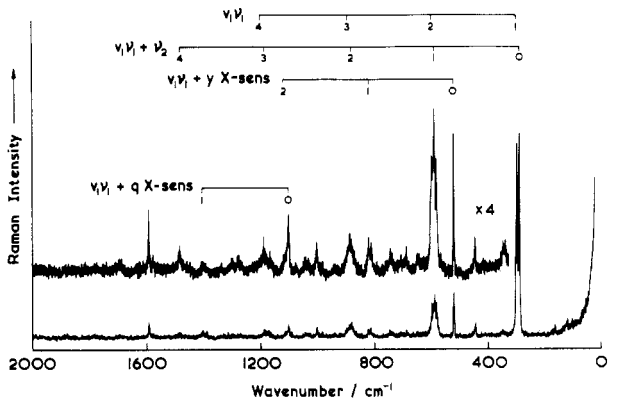

Figure 4. Resonance Raman spectrum (2000–20 cm^{-1}) of $Rh_2(O_2CC_3H_7)_4(PPh_3)_2$ as a KCl disk at ca. 80 K with 363.8-nm excitation (resolution ca. 1.5 cm^{-1}).

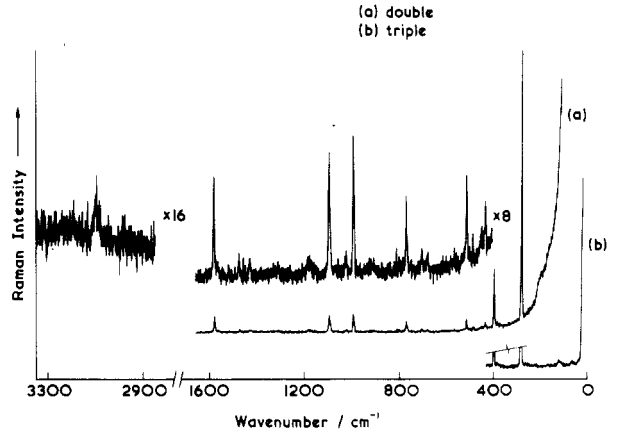

Figure 5. Raman spectrum (3350–2850 and 1650–25 cm^{-1}) of $Rh_2(O_2CH)_4(PPh_3)_2$ as a KCl disk at ca. 80 K with 514.5-nm excitation (resolution ca. 3 cm^{-1}).

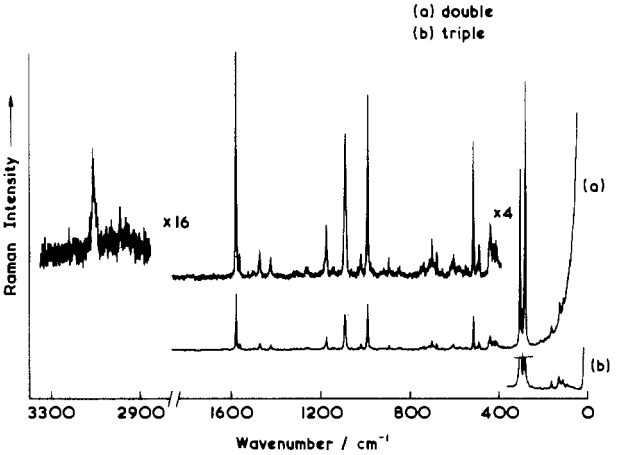

Figure 6. Raman spectrum (3325–2850 and 1900–30 cm^{-1}) of $Rh_2(O_2CC_2H_5)_4(PPh_3)_2$ as a KCl disk at ca. 15 K with 514.5-nm excitation (resolution ca. 3 cm^{-1}).

It should be noted that Miskowski et al.[25] observed an intense band ($\epsilon \approx 25000\ M^{-1}\ cm^{-1}$) in the near-UV region of the spectrum of $[Rh_2(O_2CCH_3)_4X_2]^{2-}$ (X = Cl, Br, I). This band red-shifts as the halogen becomes more reducing, viz., λ_{max} occurs at 272, 291, and 332 nm for X = Cl, Br, and I, respectively, and is thus predominantly σ(RhX) $\rightarrow$ $\sigma^*(Rh_2)$ in character.

Raman Spectra. The resonance Raman spectra for the complexes $Rh_2(O_2CR)_4(PPh_3)_2$ with R = H, C_2H_5, and C_3H_7 are shown in Figures 2–4, respectively. It was not possible to obtain a spectrum of $Rh_2(O_2CH)_4(PPh_3)_2$ with 363.8-nm excitation owing

(24) Clark, R. J. H.; Hempleman, A. J.; Dawes, H. M.; Hursthouse, M. B.; Flint, C. D. *J. Chem. Soc., Dalton Trans.* **1985**, 1775.

(25) Miskowski, V. M.; Schaefer, W. P.; Sadeghi, B.; Santarsiero, B. D.; Gray, H. B. *Inorg. Chem.* **1984**, *23*, 1154.

Table II. Wavenumbers (cm^{-1}) of Bands Observed in the Resonance Raman Spectrum[a] of $[Rh_2(O_2CC_2H_5)_4(PPh_3)_2]$ at ca. 15 K

$\tilde{\nu}$	assignt	$\tilde{\nu}$	assignt
287 vs	ν_1, ν(RhRh)	1071 vw	d β(CH)
310 s	ν_2, ν(RhO)	1098 w	q X-sens
322 w	ν(RhO)	1117 vw	$\nu_1 + \nu_2$ + y X-sens
417 vw	t X-sens	1167 vw	$3\nu_1 + \nu_2$
427 vw		1183 vw	a β(CH)
447 vw		1193 vw	$2\nu_1 + 2\nu_2$
521 m	y X-sens	1265 vw	e β(CH)
573 m	$2\nu_1$	1276 vw	
579 w, sh		1286 vw	ν_1 + p-ring
596 m	$\nu_1 + \nu_2$	1305 vw	ν_2 + p-ring
619 w	$2\nu_2$	1384 vw	ν_1 + q X-sens
686 vw	r X-sens	1406 vw	ν_2 + q X-sens
710 vw, br	ν_1 + t X-sens	1433 vw	n ν(CC)
808 w	ν_1 + y X-sens	1478 vw	m ν(CC)
831 w	ν_2 + y X-sens	1570 vw	l ν(CC)
859 w	$3\nu_1$	1587 vw	k ν(CC)
881 w	$2\nu_1 + \nu_2$	1620 vw	y X-sens + q X-sens
904 vw	$\nu_1 + 2\nu_2$	1765 vw	ν_1 + m ν(CC)
930 vw	$3\nu_2$	1872 vw	ν_1 + k ν(CC)
972 vw	ν_1 + r X-sens	1898 vw	ν_2 + k ν(CC)
998 w	p-ring	2168 vw, br	$2\nu_1$ + k ν(CC)

[a] 363.8-nm excitation.

Table III. Wavenumbers (cm^{-1}) of Bands Observed in the Resonance Raman Spectrum[a] of $[Rh_2(O_2CC_3H_7)_4(PPh_3)_2]$ at ca. 15 K

$\tilde{\nu}$	assignt	$\tilde{\nu}$	assignt
119 vw		868 w, sh	$3\nu_2$
130 vw		877 w	$\nu_1 + 2\nu_2$
162 w		885 w	$2\nu_1 + \nu_2$
201 vw		895 w	$3\nu_1$
279 vw		975 vw	h γ(CH)/ν_2 + r X-sens
289 vs	ν_2, ν(RhO)	996 vw, sh	j γ(CH)
295 m, sh		1001 w	p-ring
299 vs	ν_1, ν(RhRh)	1031 vw	b β(CH)
340 vw		1040 vw	
349 vw		1100 w	q X-sens/$2\nu_2$ + y X-sens
406 vw	w ϕ(CC)	1108 vw	$\nu_1 + \nu_2$ + y X-sens
419 vw	t X-sens	1118 vw	$2\nu_1$ + y X-sens
446 w		1162 vw	
459 vw		1174 vw	$2\nu_1 + 2\nu_2$
517 w, sh	y X-sens	1186 vw	$3\nu_1 + \nu_2$/a β(CH)
520 m		1195 vw	$4\nu_1$
579 m	$2\nu_2$	1278 vw	e β(CH)
588 m	$\nu_1 + \nu_2$	1290 vw	ν_2 + p-ring
597 m	$2\nu_1$	1300 vw	ν_1 + p-ring
605 vw		1399 vw, br	ν_1 + q X-sens
648 vw		1454 vw	
687 vw	r X-sens	1482 vw, br	$4\nu_1 + \nu_2$
707 vw		1571 vw	l ν(CC)
734 vw	ν_2 + t X-sens	1588 w	k ν(CC)
744 vw	ν_1 + t X-sens	1685 vw, br	$\nu_1 + \nu_2$ + q X-sens
756 vw	f γ(CH)	1694 vw, br	$2\nu_1$ + q X-sens
810 w	ν_2 + y X-sens	1886 vw	ν_1 + k ν(CC)
820 w	ν_1 + y X-sens		

[a] 363.8-nm excitation.

to sample decomposition; to reduce this, 406.7-nm excitation was used since the molar absorptivity is much less at this wavelength. Band listings and assignments are given in Tables I–III for the formate, propionate, and butyrate complexes, respectively. Bands at 286, 289,[12,13] 287, and 299 cm^{-1} for the complexes with R = H, CH_3, C_2H_5, and C_3H_7, respectively, are assigned to ν_1 (ν(RhRh)), whereas those at 402, 338,[12,13] 310, and 289 cm^{-1}, respectively, are assigned to the totally symmetric fundamental ν_2 (ν(RhO)). The assignment of ν(RhRh) (with the exception of the case where R = CH_3, which is rendered certain by isotopic data)[13] is made on the bases that ν(RhRh) gives rise to (a) the strongest band in the off-resonance (514.5-nm) spectra and (b) the most and longest combination band progressions in the resonance Raman spectra (Figures 5–7). For the butyrate it is particularly difficult to distinguish ν_1 from ν_2 (in the absence of isotopic data) since they are almost accidentally degenerate; in this case it appears that $\nu_1 > \nu_2$, the reverse of the situation that exists for the other three complexes. Clearly, the variation in ν_1 over the four complexes is $\lesssim$13 cm^{-1} (cf. that for the diruthenium complexes is 12 cm^{-1})[9] whereas that in ν_2 is much larger than this; moreover, ν_2 falls (as expected on ligand mass grounds) progressively with increasing mass of R despite the near-constancy of the Rh–O distance.[26] Indeed, the wavenumber dependence of ν_2 rather closely follows that expected on the basis of a simple diatomic model in which the rhodium atom vibrates against an entity of mass equal to that of the entire carboxylate group, viz. for acetate and ν_2 = 338 cm^{-1} as marker, the calculated (observed)

Table IV. Wavenumbers (cm^{-1}) of Bands Observed in the Raman Spectrum[a] of $[Rh_2(O_2CH)_4(PPh_3)_2]$ at ca. 80 K

$\tilde{\nu}$	assignt	$\tilde{\nu}$	assignt
68 vw		816 vw	
123 vw, br		995 w, sh	j γ(CH)
265 vw	u X-sens	999 w	p-ring
286 vs	ν_1, ν(RhRh)	1028 vw	b β(CH)
389 vw	ν(RhO)	1100 w	q X-sens
402 m	ν_2, ν(RhO)	1186 vw	a β(CH)
440 vw	t X-sens	1436 vw	n ν(CC)
492 vw		1482 vw	m ν(CC)
520 w	y X-sens	1524 vw	
684 vw	r X-sens	1587 vw	k ν(CC)
691 vw	v ϕ(CC)	3102 vw	
775 w	δ(OCO)	3114 vw	1524 + 1587

[a] 514.5-nm excitation.

Table V. Wavenumbers (cm^{-1}) of Bands Observed in the Raman Spectrum[a] of $[Rh_2(O_2CC_2H_5)_4(PPh_3)_2]$ at ca. 15 K

$\tilde{\nu}$	assignt	$\tilde{\nu}$	assignt
36 vw		851 vw	g γ(CH)
63 vw		860 vw	
95 vw		897 vw, sh	ν(CC)
115 w		903 vw	
130 w		969 vw	h γ(CH)
167 w		977 vw	
219 vw		986 vw	j γ(CH)
255 vw	u X-sens	992 vw	
272 vw, sh		998 m	p-ring
278 w, sh		1003 w, sh	
287 vs	ν_1, ν(RhRh)	1008 vw, sh	ρ(CH_3)
310 s	ν_2, ν(RhO)	1013 vw	
320 w, sh	ν(RhO)	1028 w	b β(CH)
333 vw		1030 vw	
396 vw	w ϕ(CC)	1072 vw	d β(CH)
404 vw		1098 m	q X-sens
416 w	t X-sens	1151 vw	c β(CH)
430 w		1158 vw	
444 w		1183 w	a β(CH)
449 w		1191 vw, sh	
494 w, sh	y X-sens	1266 vw	e β(CH)
496 w		1276 vw	
505 vw		1312 vw	
521 m		1330 vw	
547 vw		1387 vw	2v
557 vw		1432 w	n ν(CC)
587 vw	in-plane ρ_r(COO)	1438 vw, sh	
610 vw		1480 w	m ν(CC)
618 vw	s α(CCC)	1485 vw	
624 vw, sh	out-of-plane ρ_w(COO)	1510 vw, br	
661 vw		1571 w	l, ν(CC)
671 vw		1578 vw	
685 vw	r X-sens	1587 m	k ν(CC)
695 vw	v ϕ(CC)	1783 vw	
708 w	δ(OCO)	1804 vw	
720 vw		2920 vw	ν(CH) aliphatic
744 vw		2960 vw	
749 vw	f γ(CH)	2990 vw	
753 vw		3105 w, br	
759 vw		3220 vw	

[a] 514.5-nm excitation.

(26) Koh, Y. B.; Christoph, G. G. *Inorg. Chem.* **1979**, *18*, 1122.

Table VI. Wavenumbers (cm^{-1}) of Bands Observed in the Raman Spectrum[a] of $[Rh_2(O_2CC_3H_7)_4(PPh_3)_2]$ at ca. 80 K

$\tilde{\nu}$	assignt	$\tilde{\nu}$	assignt
48 vw		709 w	δ(OCO)
68 w		719 vw	
85 w, sh		737 vw, sh	
94 w, sh		744 vw	f γ(CH)
102 w		755 vw	
121 w, sh		852 vw	g γ(CH)
129 w		874 vw	
161 w		895 vw	ν(CC)
175 vw		938 vw	
200 vw		957 vw	
217 vw	x X-sens	995 w, sh	j γ(CH)
234 vw		998 w, sh	p-ring
255 vw		1001 w	
267 vw	u X-sens	1028 vw	b β(CH)
273 vw		1075 vw	d β(CH)
290 s	ν_2, ν(RhO)	1100 m	q X-sens
299 vs	ν_1, ν(RhRh)	1155 vw	c β(CH)
323 vw		1187 w	a β(CH)
339 vw	ν(RhO)	1196 vw, sh	
345 vw		1434 vw	n ν(CC)
392 vw	w φ(CC)	1437 vw, sh	
406 vw		1482 vw	m ν(CC)
420 vw		1488 vw, sh	
444 w, sh	t X-sens	1500 vw	
447 m		1572 vw	l ν(CC)
461 vw		1588 m	k ν(CC)
498 w		2870 vw	
502 w	y X-sens	2900 vw, br	ν(CH) aliphatic
520 w		2930 vw, br	
584 vw	in-plane ρ_r(COO)	3005 vw	
605 vw		3045 vw, sh	ν(CH) aromatic
637 vw	out-of-plane ρ_w(COO)	3060 vw	
688 vw	r X-sens	3175 vw	2k
696 vw	v φ(CC)		

[a] 514.5-nm excitation.

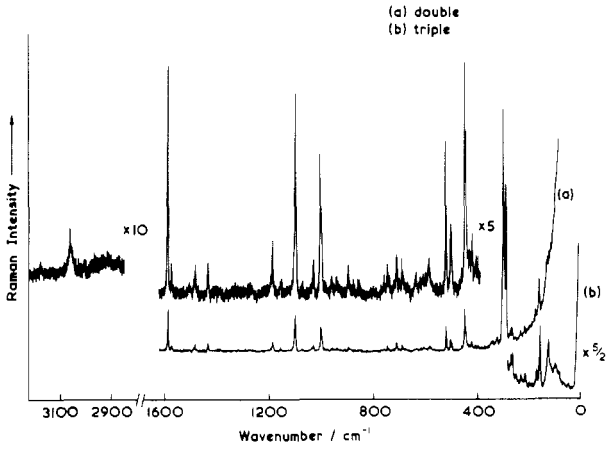

Figure 7. Raman spectrum (3200–2850 and 1630–20 cm^{-1}) of $Rh_2(O_2CC_3H_7)_4(PPh_3)_2$ as a KCl disk at ca. 80 K with 514.5-nm excitation (resolution ca. 3 cm^{-1}).

wavenumbers (cm^{-1}) for ν_2 for the other carboxylates are as follows: formate, 387 (402); (^{18}O)acetate,[12,13] 330 (332); propionate, 304 (310); butyrate, 278 (289).

One puzzling matter is that ν(RhP) might also be expected to be enhanced at resonance with the ca. 370 nm band owing to the fact that PRhRhP is linear, yet no band could be identified as such, either on or off resonance. As argued elsewhere,[12,13] on both mass and bond length grounds, ν(RhP) must occur at a low wavenumber, probably well below 200 cm^{-1}. The reason for the very low transition polarizability for ν(RhP) is not clear, but the result speaks for little if any involvement of phosphorus orbitals in the resonant electronic transition.

The relative intensities of the ν_1 and ν_2 bands, $I(\nu_2)/I(\nu_1)$, are also of interest. These increase in the order R = H < CH_3 < C_2H_5 < C_3H_7 as the wavenumber separation, $\nu_2 - \nu_1$, decreases. ^{18}O

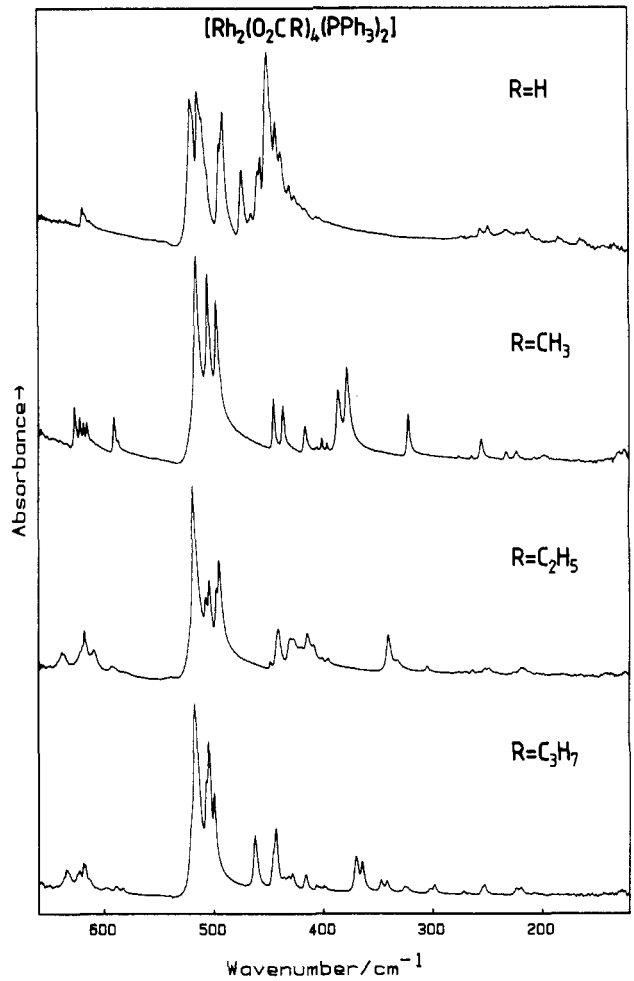

Figure 8. FTIR spectra (660–140 cm^{-1}) of $Rh_2(O_2CR)_4(PPh_3)_2$ (R = H, CH_3, C_2H_5, C_3H_7) as wax disks at ca. 80 K.

isotopic work[12,13] on $Rh_2(O_2CCH_3)_4(PPh_3)_2$ has clearly demonstrated that the RhO and RhRh symmetry coordinates are almost mechanically uncoupled. Any coupling that does occur will have the (very slight) effect of lowering ν_1 for the formate, acetate, and propionate but of raising it for the butyrate. The intensity result must, however, imply the presence of increased and significant electronic coupling between ν_2 and ν_1 as these approach accidental degeneracy in the case where R = C_3H_7. Such coupling is well-known to yield much greater effects on band intensities than on band wavenumbers; indeed, $I(\nu_2)/I(\nu_1)$ is even significantly different for $Rh_2(^{16}O_2CCH_3)_4(PPh_3)_2$ and $Rh_2(O_2CCD_3)_4(PPh_3)_2$, on account of $\nu_2 - \nu_1$ being 49 cm^{-1} in the first case but only 38 cm^{-1} in the second.[13] Similar effects have been observed for $Ru_2(O_2CR)_4Cl$.[9] The exact quantification of this coupling is not straightforward because (a) the value of $I(\nu_2)/I(\nu_1)$ varies with excitation wavelength in each case and (b) 514.5-nm excitation is not at a constant-wavenumber separation from λ_{max} for all complexes[9] owing to the R group dependence of λ_{max}.

As shown for $Mo_2(O_2CCH_3)_4$,[4,27] $Os_2(O_2CCH_3)_4Cl_2$,[28] and several dirhodium tetraacetate complexes,[12,14] bands assigned to ν(MO) show large shifts upon acetate deuteriation and hence involve considerable contributions from methyl symmetry coordinates. Obviously, changing the R group will affect the polarizability and thus the intensity of this band in the Raman spectrum. Consequently, the intensity variation in ν(MO) bands with alkyl group could also arise in part from a change in alkyl group components to the normal mode.

(27) Hempleman, A. J.; Clark, R. J. H.; Flint, C. D. *Inorg. Chem.* **1986**, *25*, 2915.
(28) Clark, R. J. H.; Hempleman, A. J.; Tocher, D. A. *J. Am. Chem. Soc.* **1988**, *110*, 5968.
(29) Clark, R. J. H.; Franks, M. L. *J. Chem. Soc., Dalton Trans.* **1976**, 1825.

Table VII. Wavenumbers (cm^{-1}) of Bands Observed in the Far-Infrared (660–40 cm^{-1}) Spectra of the Complexes $Rh_2(O_2CR)_4(PPh_3)_2$ (R = H, CH_3, C_2H_5, C_3H_7) at ca. 80 K

H		CH_3[a]		C_2H_5		C_3H_7	
$\tilde{\nu}$	assignt	$\tilde{\nu}$	assignt	$\tilde{\nu}$	assignt	$\tilde{\nu}$	assignt
619 vw	s α(CCC)	627 w	out-of-plane ρ_w(COO)	638 vw	out-of-plane ρ_w(COO)	636 w	out-of-plane ρ_w(COO)
616 vw		622 w		622 vw		623 w	
519 m		619 vw	s α(CCC)	618 vw	s α(CCC)	619 vw	s α(CCC)
517 m, sh		616 vw		610 vw		617 vw	
513 m		591 vw	in-plane ρ_r(COO)	594 vw	in-plane ρ_r(COO)	614 vw, sh	
510 m	y X-sens	587 vw		517 s		599 vw	
505 w, sh		515 m	y X-sens	507 m	y X-sens	589 vw	in-plane ρ_r(COO)
494 m		504 m		504 m		583 vw	
490 m		497 m		497 m		520 w, sh	y X-sens
473 w	ν(RhO)	494 w, sh		495 m		515 m	
464 vw		444 w		449 vw		506 m	
458 w	ν(RhO)	436 w	t X-sens	443 vw, sh	t X-sens	503 m	
456 m		416 vw		441 vw		499 m	
449 m		408 vw		431 vw		461 w	
442 m	t X-sens + ν(RhO)	405 vw	w ϕ(CC)	428 vw		445 w, sh	t X-sens
437 m		400 vw		422 vw		442 w	
429 w		396 vw		415 vw		436 vw	
425 w		385 w	ν(RhO)	409 vw		431 vw	
420 vw		377 w		402 vw	w ϕ(CC)	427 vw	
415 vw		321 w		398 vw		415 vw	
404 vw	w ϕ(CC)	275 vw	u X-sens	396 vw		406 vw	w ϕ(CC)
402 vw		264 vw		341 vw	ν(RhO)	404 vw	
255 vw	u X-sens	255 vw		333 vw		402 vw	
248 vw		232 vw	x X-sens	306 vw		399 vw	
231 vw	x X-sens	222 vw		278 vw	u X-sens	397 vw	
212 vw		207 vw	δ(ORhO) or δ(RhRhO)	265 vw		369 w	ν(RhO)
183 vw		197 vw		253 vw		364 w	
162 vw		130 vw		249 vw		347 vw	
132 vw		124 vw		227 vw	x X-sens	341 vw	
		110 vw		219 vw		325 vw	
				213 vw		323 vw, sh	
				141 vw		302 vw	
				125 vw		298 vw	
				112 vw		272 vw	u X-sens
				100 vw		270 vw	
						267 vw	
						254 vw, sh	
						253 vw	
						224 vw	x X-sens
						219 vw	
						128 vw	

[a] Data taken from ref 13.

The overtone and combination bands observed in the resonance Raman spectra of each complex are similar to one another, band progressions in ν_1 reaching $4\nu_1$, $4\nu_1$, $3\nu_1$, and $4\nu_1$ for the complexes with R = H, CH_3, C_2H_5, and C_3H_7, respectively, and in ν_2 reaching ν_2, $2\nu_2$, $3\nu_2$, and $3\nu_2$, respectively. The lengths of the observed progressions in ν_2 are evidently a function of the separation ν(RhO) − ν(RhRh); cf. the similar situation for the series $Ru_2(O_2CR)_4Cl$.[9,11]

In the resonance Raman spectra, ν_1 forms a variety of progressions based upon one (and also, occasionally, two) quanta of one of the other Raman-active modes. This is most obvious where the other mode is ν_2, but short progressions of this sort are also observed for certain of the X-sensitive ring modes, viz. y (an out-of-plane bend), q (largely a P–C stretch) and k (largely a C–C stretch). Why these particular ring modes rather than others become involved in combination band progressions is not clear, but the result implies that there must be small structural changes on excitation to the resonant excited state along these coordinates in addition to larger ones along ν_1.

Infrared Spectra. Assignments for the infrared-active ν(RhO) modes are less clear than for the Raman-active modes. For $Rh_2(O_2CCH_3)_4(PPh_3)_2$, bands at 385, 377, and 321 cm^{-1} have already been assigned to ν(RhO)[13] by use of ^{18}O and CD_3 isotopomers. The infrared-active ν(RhO) bands are at higher wavenumber than their Raman-active counterparts; cf. those of $Mo_2(O_2CCH_3)_4$.[3,4,27] The 80 K far-infrared spectra for the complexes $Rh_2(O_2CR)_4(PPh_3)_2$ (R = H, CH_3, C_2H_5, C_3H_7) are shown in Figure 8. For $Rh_2(O_2CH)_4(PPh_3)_2$ there are clearly no bands in the 400–300-cm^{-1} region and, by comparison with the Raman spectrum, ν(RhO) would be expected to lie somewhere above 400 cm^{-1}; cf. the assignments of Kharitonov et al.[30] for $Rh_2(O_2CH)_4(H_2O)_2$ (499, 483, 460, and 455 cm^{-1}). Bands at 473, 449, and 429 cm^{-1} in the infrared spectrum of $Rh_2(O_2CH)_4(PPh_3)_2$ are assigned to ν(RhO), although this assignment remains tentative as there is considerable overlap with the X-sensitive bands of the axial ligand.[16] For $Rh_2(O_2CC_2H_5)_4(PPh_3)_2$ and $Rh_2(O_2CC_3H_7)_4(PPh_3)_2$, bands at 341, 333, and 306 cm^{-1} and at 369, 364, 347, and 341 cm^{-1}, respectively, are assigned to ν(RhO).

Table VII contains band listings and band assignments for the infrared spectra of all four complexes at 80 K in the range 660–40 cm^{-1}; full band listings and assignments (3500–40 cm^{-1}) for the R = H, C_2H_5, and C_3H_7 complexes are included in the supplementary material (Tables VIII–X).

The only band due to the carboxylate group that can be assigned confidently is ν_{as}(COO), which is found at 1611, 1595, 1592, and 1592 cm^{-1} for R = H, CH_3, C_2H_5, and C_3H_7, respectively. The assignment of ν_s(COO) is less clear owing to its dependence on the mass of the R group.[31]

Conclusion

While ν_1 (ν(RhRh)) for $Rh_2(O_2CR)_4(PPh_3)_2$ at 292 ± 7 cm^{-1} is virtually insensitive to a change of R group, ν_2 (ν(RhO)) is highly

(30) Kharitonov, Yu. Ya.; Mazo, G. Ya.; Knyazeva, N. A. *Russ. J. Inorg. Chem. (Engl. Transl.)* **1970**, *15*, 739.
(31) Spinner, E. *J. Chem. Soc.* **1964**, 4217.

sensitive to such a change, ranging from 402 cm^{-1} (R = H) to 289 cm^{-1} ($R = C_3H_7$). This sensitivity of ν(RhO) to R is surprising, bearing in mind the presumed near-constancy of the Rh–O bond length (cf. for six diruthenium tetracarboxylate complexes, the Ru–O distance is 2.01 ± 0.01 Å)[32] in such complexes, a result that calls into question the uncritical usage of the simple empirical relationship between metal–metal force constant and bond length more widely to metal–oxygen bonds.[33]

Supplementary Material Available: Tables VIII–X, giving infrared data for $[Rh_2(O_2CH)_4(PPh_3)_2]$, $[Rh_2(O_2CC_2H_5)_4(PPh_3)_2]$, and $[Rh_2(O_2CC_3H_7)_4(PPh_3)_2]$, respectively (6 pages). Ordering information is given on any current masthead page.

(32) Bino, A.; Cotton, F. A.; Felthouse, T. R. *Inorg. Chem.* **1979**, *18*, 2599.

(33) Miskowski, V. M.; Dallinger, R. F.; Christoph, G. G.; Morris, D. E.; Spies, G. H.; Woodruff, W. H. *Inorg. Chem.* **1987**, *26*, 2127.

Contribution from the Chemistry Department, University of Tasmania, Box 252C, Hobart, Tasmania 7001, Australia

Analysis of the Vibrational Fine Structure in the Electronic Spectrum of the Planar $CuCl_4^{2-}$ Ion in *N*-(2-Ammonioethyl)morpholinium Tetrachlorocuprate(II): Evidence for a Pseudotetrahedral Distortion in the $^2A_{1g}$ Excited Electronic State

Robbie G. McDonald, Mark J. Riley, and Michael A. Hitchman*

Received May 3, 1988

The electronic spectrum of the planar $CuCl_4^{2-}$ ion in *N*-(2-ammonioethyl)morpholinium tetrachlorocuprate(II) is reported. The temperature dependence of the band maximum of the $^2A_{1g}(z^2) \leftarrow {}^2B_{1g}(x^2 - y^2)$ transition suggests that the excited-state potential surface is distorted in the β_{2u} out-of-plane bending vibration, with energy minima corresponding to two equivalent pseudotetrahedral geometries. However, the distortion from planarity is somewhat less than that proposed for the $^2A_{1g}(z^2)$ excited state of planar $CuCl_4^{2-}$ in other lattices. The vibrational fine structure in the spectrum is consistent with an excited-state potential surface of this form, being incompatible with the simple model of vibronic coupling normally used to interpret Laporte-forbidden electronic transitions.

Introduction

Detailed analysis of the electronic spectra of transition-metal complexes can provide information that is of value in several areas of chemistry.[1] Simple, planar ions of the type MX_4^{2-}, where M is Pd, Pt, or Cu and X is a halide, have been particularly important in this respect.[2-7] The low-temperature spectra of platinum(II) and palladium(II) chloride and bromide complexes show extensive fine structure, and analysis of this fine structure has provided a detailed picture of the nature of the vibrations inducing the intensity of the d–d transitions and the change in metal–ligand bond lengths accompanying the electronic excitations.[2] The spectrum of planar $CuCl_4^{2-}$ is unusual for a number of reasons. Some bands increase dramatically in intensity as the temperature is raised from 10 to 290 K, and it has been inferred from this that the out-of-plane bending vibration is of very low energy.[3,4] Also, the band maxima exhibit an anomalous red shift of up to ~900 cm^{-1} over the same temperature range, and in a recent study,[5] it was shown that this implies that the complex has a potential surface with double minima corresponding to two equivalent pseudotetrahedral coordination geometries in each excited electronic state. For one compound this was confirmed by the analysis of a system of "hot" bands.[7] The extent of the vibrational fine structure resolved in the spectrum of planar $CuCl_4^{2-}$ at low temperature varies markedly from one crystal lattice to another. This fine structure has previously been interpreted by using the conventional model of vibronic coupling, with differences between the compounds being ascribed to coupling with different lattice modes.[3,4] However, if, as has been proposed, the potential surfaces of the excited electronic states differ from that in the ground state in an intensity-inducing normal mode, then simple vibronic selection rules will break down. Moreover, it has been pointed out that the extent of the distortion in the excited state may well be lattice dependent,[5,7] which could explain why the fine structure differs from one compound to another.

The compound *N*-(2-ammonioethyl)morpholinium tetrachlorocuprate(II), (Naem)$CuCl_4$, is unusual in that the green modification contains $CuCl_4^{2-}$ ions of two kinds, one having a distorted tetrahedral geometry and the other a planar geometry.[8] Recently, we presented an interpretation of the band energies and intensities of the distorted tetrahedral complex using the angular overlap model.[6] The molecular spectrum of the planar complex in (Naem)$CuCl_4$ shows well-resolved vibrational fine structure for the $^2A_{1g}(z^2) \leftarrow {}^2B_{1g}(x^2 - y^2)$ transition, the nature of which is quite incompatible with the simple model of vibronic intensity stealing in which the ground and excited states have identical potential surfaces except for a displacement in modes of α_{1g} symmetry. It is the subject of the present paper to show that these spectra are consistent with a model in which the excited state has a potential surface distorted in the β_{2u} normal vibration to give two equivalent minima, each corresponding to a coordination geometry distorted slightly from planarity.

Experimental Section

The preparation and characterization of crystals of the green form of (Naem)$CuCl_4$ have been described previously.[6,8] Spectra of the prominent (10$\bar{1}$) crystal face were recorded over a temperature range by using a Cary 17 spectrophotometer by a technique described elsewhere.[9] Typical spectra with the electric vector of polarized light parallel to the crystal extinction directions are shown in Figure 1. The samples were cooled with a Cryodyne 21 refrigerator, and the crystal thickness, which

* To whom correspondence should be addressed.

(1) For a general discussion of the spectra of transition metal complexes see: Lever, A. B. P. *Inorganic Electronic Spectroscopy*, 2nd ed.; Elsevier: Amsterdam, 1984.
(2) (a) Patterson, H. H.; Godfrey, J. J.; Khan, S. M. *Inorg. Chem.* **1972**, *11*, 2872. (b) Harrison, T. G.; Patterson, H. H.; Godfrey, J. J. *Inorg. Chem.* **1976**, *15*, 1291. (c) Yersin, H.; Otto, H.; Zink, J. I.; Gliemann, G. *J. Am. Chem. Soc.* **1980**, *102*, 951.
(3) Hitchman, M. A.; Cassidy, P. J. *Inorg. Chem.* **1979**, *18*, 1745.
(4) McDonald, R. G.; Hitchman, M. A. *Inorg. Chem.* **1986**, *25*, 3273.
(5) Riley, M. J.; Hitchman, M. A. *Inorg. Chem.* **1987**, *26*, 3205.
(6) McDonald, R. G.; Riley, M. J.; Hitchman, M. A. *Inorg. Chem.* **1988**, *27*, 894.
(7) McDonald, R. G.; Riley, M. J.; Hitchman, M. A. *Chem. Phys. Lett.* **1987**, *142*, 529.
(8) Battaglia, L. P.; Bonamartini Corradi, A.; Marcotrigiano, G.; Menabue, L.; Pellacani, G. C. *Inorg. Chem.* **1982**, *21*, 3919.
(9) Hitchman, M. A. *Transition Metal Chemistry*; Marcel Dekker: New York, 1985; Vol. 9.

0020-1669/89/1328-0752$01.50/0 © 1989 American Chemical Society